Available online at www.sciencedirect.com
SCIENCE DIRECT®
Engineering Structures 26 (2004) 1889–1904
ENGINEERING STRUCTURES
www.elsevier.com/locate/engstruct

Evaluation of reinforced connections between steel beams and box columns

Cheng-Chih Chen *, Chun-Chou Lin, Chia-Liang Tsai

Department of Civil Engineering, National Chiao Tung University, Hsinchu 30010, Taiwan

Received 7 March 2004; received in revised form 23 June 2004; accepted 25 June 2004

Abstract

This study elucidates the cyclic behaviour of connection between a steel beam and a welded box column. Distribution of stresses at the joint between beam and box column inherently differ from those of the joint to the H-shaped column, as confirmed by finite element analysis. Six large-scale specimens were designed. A specimen with an unreinforced connection was tested initially to clarify its performance. The test results indicated that brittle fracture occurs at the beam flange complete joint penetration weld and in the weld access hole region, because the stresses are concentrated in these regions. Nevertheless, specimens reinforced by vertical rib plates on beam flanges achieve an inelastic rotation of more than 3% rad prior to failure by forming a plastic hinge in the beam away from the beam-to-column interface. The test results also revealed that welding diaphragm inside the box column is crucial during the welding process to the integrity of the connection, ensuring that beam forces are transferred to the connection.

Keywords: Connection; Box column; Rib; Plastic rotation

1. Introduction

The 1994 Northridge earthquake damaged a number of beam-to-column moment connections used in steel moment-resisting frames. Engineers have queried whether moment connections can reliably ensure that the steel moment-resisting frames are sufficiently ductile. The type of moment connections sustained unexpected fractures was extensively used in practice before the Northridge earthquake. These connections are 'bolted web and welded flange' (BWWF) moment connections. Beam flanges are welded to the column flange through a complete joint penetration (CJP) groove weld in the field, and the beam web is bolted to the shear tab, which is welded to the column flange in the shop.

Failures in these pre-Northridge BWWF moment connections have been reported. Many premature brittle fractures were initiated from the CJP flange welds and the root of the weld access hole (WAH) [1], which is required to cut the beam web to enable the CJP weld to be conducted. The WAH regions were susceptible to failure due to defective welding, residual stress, stress concentration and geometric discontinuity. Despite the different sizes of the beams and columns, these connections had almost no plastic rotation capacity [2,3]. Such fractures significantly influence the responses of frames under severe earthquake shaking. Therefore, numerous experimental and analytical studies have been undertaken to improve the performance of the steel moment-resisting connections. The goal of the improvements is to develop ductile behaviour of the beam by strengthening the connections [4–7] or weakening the beam sections [8–10]. Notably, however, most of the columns used in the specimens had the shape of wide flange, with H-shaped cross section; they are hereafter referred to 'H-shaped column'.

In some countries, another type of column section is commonly used. The column has a rectangular or a square cross section, and is built-up from plates; this is the so-called 'box column'. These box columns are frequently employed in areas of high seismic risk because they have an excellent capacity to resist biaxial

* Corresponding author. Tel.: +886-3-571-2121x54915; fax: +886-3-572-7109.
E-mail address: chrischen@mail.nctu.edu.tw (C.-C. Chen).

0141-0296/$ - see front matter © 2004 Elsevier Ltd. All rights reserved.
doi:10.1016/j.engstruct.2004.06.017

bending. Nevertheless, only limited test data concerning the connections that join the steel beam to the box column are available. One of the approaches to improve the connection with the box column is to strengthen the joint using reinforcement such as cover plate, angle stiffener, T-stiffener, flat triangular stiffener or external diaphragm [11–14]. However, the box columns used in these tests are small structural steel tubes with diameters of 200–300 mm, with thin walls less than 20 mm thick. In practice, most box columns used in high-rise buildings are built-up by welding four steel plates together. Very few tests have investigated the behaviour of connections between steel beams and welded built-up box columns. Kim et al. [15,16] tested two full-scale moment connections to US box columns fabricated using pre-Northridge connection details. Test results revealed that both specimens failed by brittle fracture of CJP welds between the beam flange and the column during a story drift angle of less than 1% rad, which resulted in no plastic rotation in the connections. Chen et al. [10] tested connections with box column by reducing beam section to achieve the desired ductility. This study evaluates and improves the behaviour of connections between the beam and the welded box column, by reinforcing connections with flange rib plates. A specimen with an unreinforced BWWF connection was tested to verify the cyclic behaviour and failure mode of the connection. Furthermore, specimens with rib-reinforced connections were developed and tested to examine their hysteresis behaviour.

2. Issues concerning connection with welded box column

Welded box columns are commonly fabricated by welding four plates using a full penetration groove weld, as shown in Fig. 1. Diaphragms must be used inside the column to transfer effectively the beam forces to the column plates. However, installing such a diaphragm is inherently very difficult. A special welding process must be used to weld the diaphragms inside the box column. As depicted in Fig. 1, after a partial penetration groove weld is performed to join the diaphragm to a pair of opposite column plates, the simplified electro slag welding process with non-consumable elevating tip (SESNET) welding process is undertaken to weld the diaphragm to the other pair of column plates. The section B–B in Fig. 1 illustrates SESNET welding. Although this welding process is highly efficient, it is costly.

The delivery of the beam forces to the column within the connection is influenced by the geometry of the cross section of the column [17]. The geometry of the column section strongly affects the stress flow transferred into the beam-to-column joint, because of the different distribution of stiffness contributed from the column web. A few preliminary analytical evaluations were performed to clarify the complex behaviour in the jointed zone. Two models of unreinforced connections, with the H-shaped column or the box column, were generated and analyzed using the finite element analysis program ANSYS [18]. The effect of the column geometry on the distribution of the stresses and the plastic equivalent strains (PEEQ) in the connections were evaluated. The moment connections were modeled simply by joining the beam web directly to the column flange. However, the models incorporated the WAHs and diaphragms to assess their effect on the distribution of the stresses. Three-dimensional brick solid elements were employed to model the structural steel. Fig. 2 presents the meshes of the models. A bilinear stress–strain relation with strain-hardening behaviour was used to model the structural steel. Von Mises yield criterion was selected to define the plasticity. The tip of the beam was incrementally displaced to simulate monotonic loading.

The elementary analyses presented herein emphasize the distribution of elastic stresses and the plastic equivalent strains in the joint at the CJP weld and the WAH region because the presence of the WAH greatly affects the fracture of the beam flange [2,19,20]. Distributions of normalized longitudinal stresses at 0.5% story drift angle and PEEQ indices at 4% story drift angle, along the beam flange width at the locations of the CJP weld and the root of the WAH, are plotted in Figs. 3 and 4, respectively. The normalized longitudinal stress is defined as the normal stress, σ_{11}, normalized by the yield stress, F_y. The PEEQ index is defined as the plastic equivalent strain, which represents local strain demand, divided by the yield strain, ε_y. Moreover, the story drift angle of 0.5% was selected to study the elastic behaviour of the connection, while the story drift angle of 4% indicates that the connection undergoes required inelastic deformation. The stresses exhibited by the connection with the box column were concentrated at both edges of the beam flange groove weld. However, the connection with the H-shaped column exhibited peak local stress streaming into the center of the beam flange at the CJP weld, as shown in Fig. 3(a). Similar analytical results were observed by Kim et al. [15]. The distinct distributions of the stresses at the CJP weld are attributed primarily to the stiffness provided by the column web, because the box column has two webs on both sides whereas the H-shaped column has only one web through the center of its cross section. PEEQ indices at 4% story drift angle shown in Fig. 4(a) demonstrated identical distribution as that of longitudinal stresses. Distributions of the longitudinal stresses along the beam flange width at the root of the WAH are shown in Fig. 3(b), and PEEQ indices are plotted in Fig. 4(b). Both connections, with the box

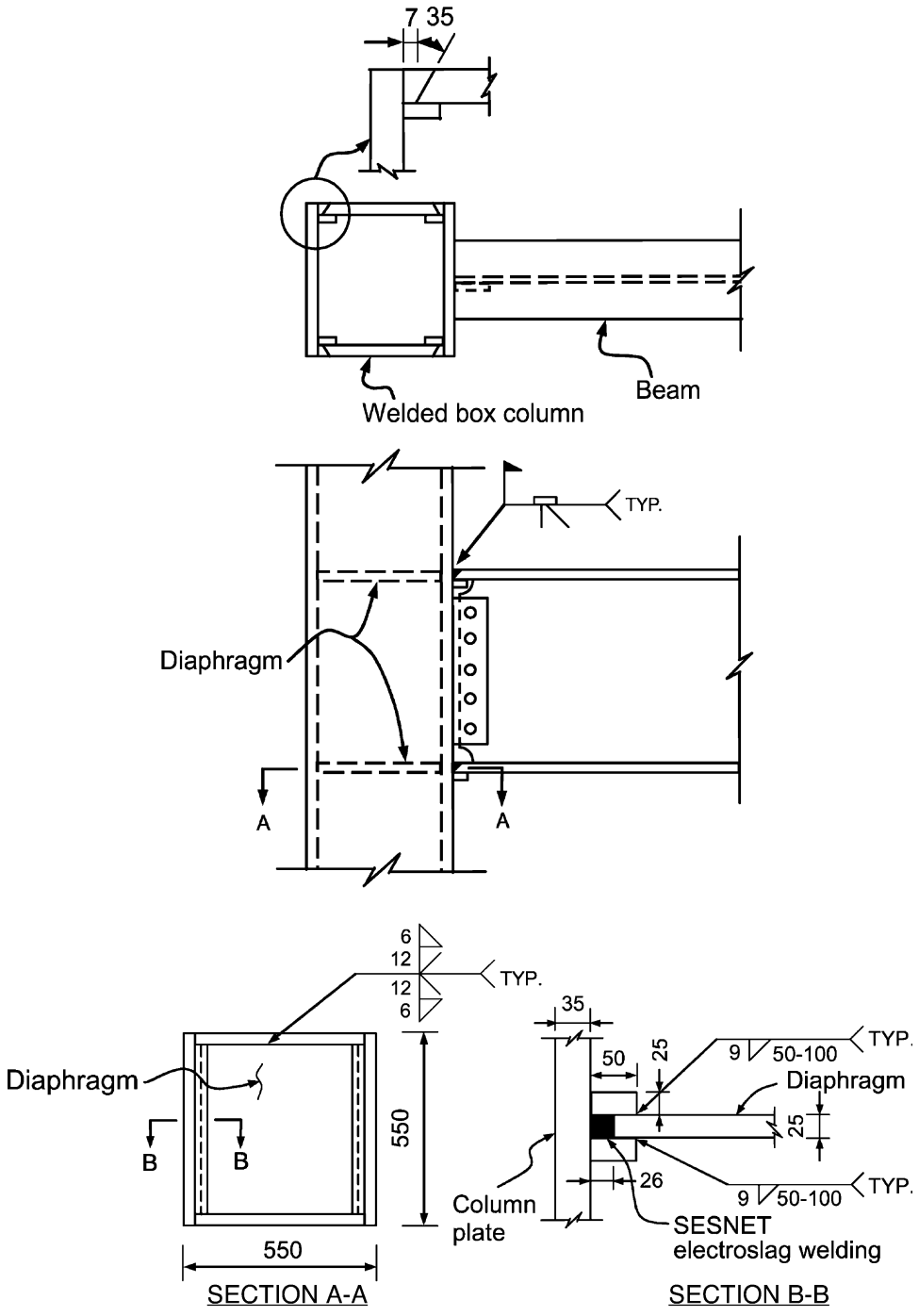

Fig. 1. Moment connection between steel beam and welded box column.

column or the H-shaped column, display localized stress concentration at the center of the beam flange, where the geometry changes abruptly. The presence of these stress concentrations results in peak local plastic strain at the CJP weld and the root of the WAH, increasing the potential to fracture at these critical locations. The stresses and plastic strains of the connections with the box column or the H-shaped column were differently distributed, so large-scale tests were conducted to investigate the performance of the connection with the box column.

3. Experimental program

An experiment was carried out to investigate the behaviour and the failure mode of connections with

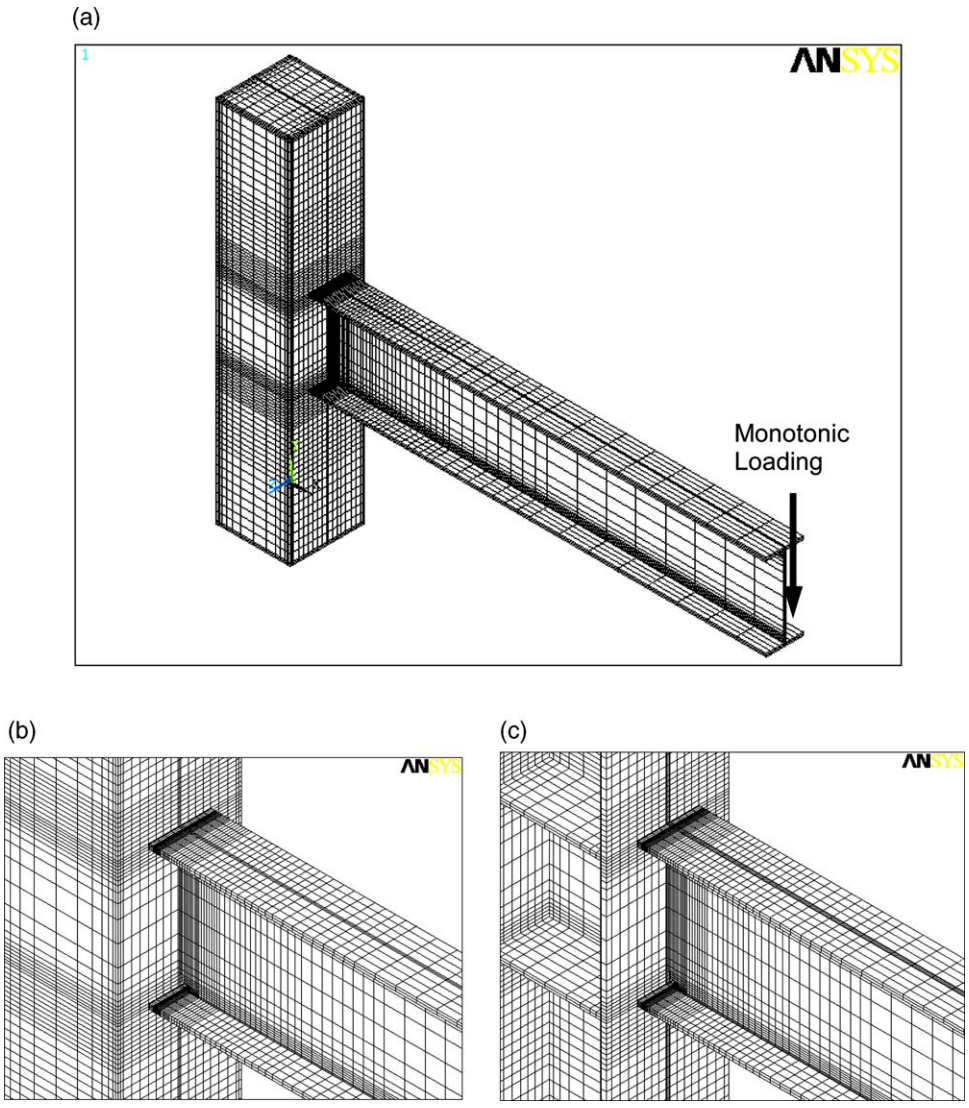

Fig. 2. Analytical models of unreinforced connections: (a) three-dimensional finite element mesh; (b) Box column connection; (c) H-shaped column connection.

the welded box column. The test began with a specimen with an unreinforced connection. Based on the behaviour and failure mode of the unreinforced connection, a series of tests were conducted on improved specimens to elucidate the effect of the reinforcement on the hysteresis behaviour.

3.1. Test specimens

A total of six large-scale specimens were designed to simulate an exterior T-shaped joint subassembly. Each subassembly contained a column between the mid-height of the two adjacent floors and a half-span of the beam. The joint from the steel beam to the box column was a BWWF moment connection. All specimens were constructed with a H700 × 300 × 13 × 24 (mm) beam and a built-up □550 × 550 × 35 × 35 (mm) box column, to reduce the influence of the size of the beam and the column on the connection behaviour. The width-thickness ratios of the beam flange and the web are 6.25 and 47.38, respectively, and the beam section categorizes to a compact section, which is capable of developing the fully plastic stress distribution. The size of the beam is approximately that of a W-shaped section, between W27 × 114 and W27 × 146, as used in the US [21]. Table 1 summarizes these six test specimens. A WAH is needed to proceed with the full penetration groove welding between the beam flange and the column flange. Fig. 5 shows the geometry of the WAH used in the specimens.

3.1.1. Specimen with unreinforced connection

Specimen BUN was fabricated without any reinforcement to investigate the performance of the BWWF moment connection with a box column. Fig. 6

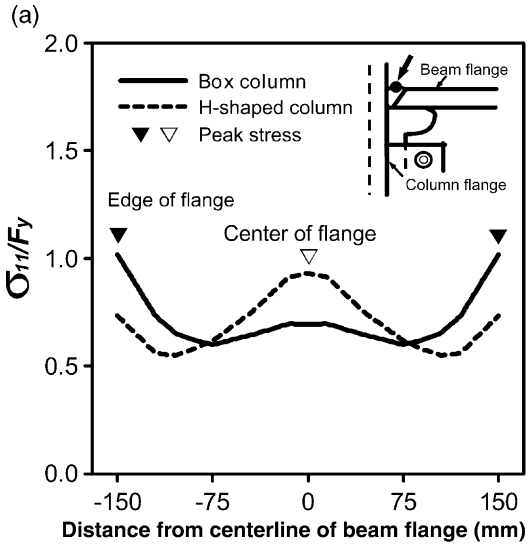

Fig. 3. Distributions of normalized longitudinal stresses along beam flange width at 0.5% story drift angle: (a) at CJP weld; (b) at root of weld access hole.

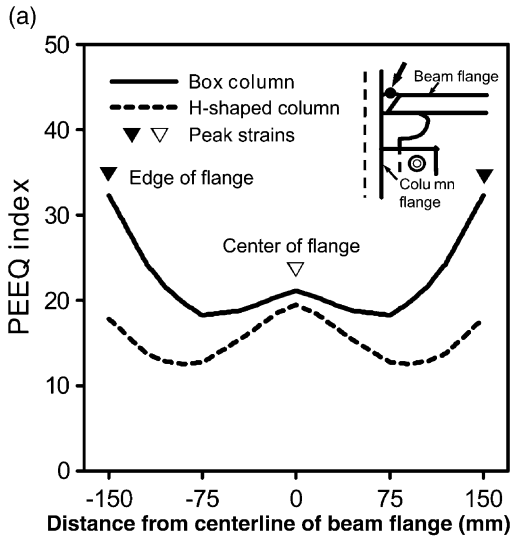

Fig. 4. Distributions of PEEQ indices along beam flange width at 4% story drift angle: (a) at CJP weld; (b) at root of weld access hole.

presents the connection details of specimen BUN, using the pre-Northridge connection details in the beam.

3.1.2. Rib reinforcing scheme

Specimen BUN failed in a brittle manner (to be discussed in Section 4.1.1), so an attempt was made to improve the connection behaviour by strengthening the connection. Tapered rib plate was used to reinforce the connection as tested by Popov and Tsai [22], Engelhardt et al. [23], and Anderson and Duan [24]. Their test results showed that connections reinforced with tapered ribs might develop stable hysteretic behaviour. Chen et al. [25] used a modified rib to

Table 1
Summary of test specimens

Specimen[a]	M_{cap}/M_{dem} at interface	Rib size (mm)	Backing bar	Note
BUN	–	–	Steel	
BR115SB	1.15	PL22 × 135 × 685	Steel	
BR105SB	1.05	PL22 × 100 × 685	Steel	
BR115SB-FW	1.15	PL22 × 135 × 685	Steel	Extra fillet weld at backing bars
BR115CB	1.15	PL25 × 135 × 790	Ceramic	
BR120CB-WP	1.20	PL25 × 150 × 790	Ceramic	Additional flat wing plates

[a] All specimens consist of a H700 × 300 × 13 × 24 (mm) beam and a □550 × 550 × 35 × 35 (mm) column.

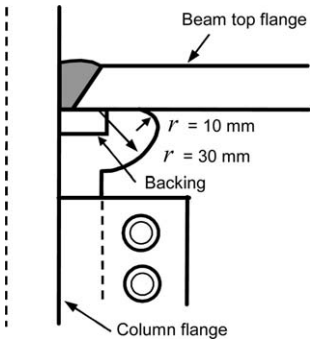

Fig. 5. Details of weld access hole.

strengthen the connection, and have proven experimentally and analytically that the connection possesses stable inelastic behaviour. However, all the specimens tested consist of an H-shaped column, and the application of the rib plate to the connection with the box column remains unknown.

The modified rib was adopted in this study. Fig. 7 shows the configuration of the connection with a welded built-up box column, in which a vertical lengthened rib plate was welded to the joint on each beam flange along the centerline. Fig. 8 illustrates the purpose of the design of the flange rib; the figure shows a cantilever of the half-span of the beam in a moment-resisting frame under a seismic force. The flexural capacity of the beam and the moment demand gradient are plotted in the figure. Full plastification of the section can develop at the intersection of the capacity line with moment demand. Hence, the plastic hinge will form away from the face of the column to ensure that the beam deforms inelastically. Moreover, the

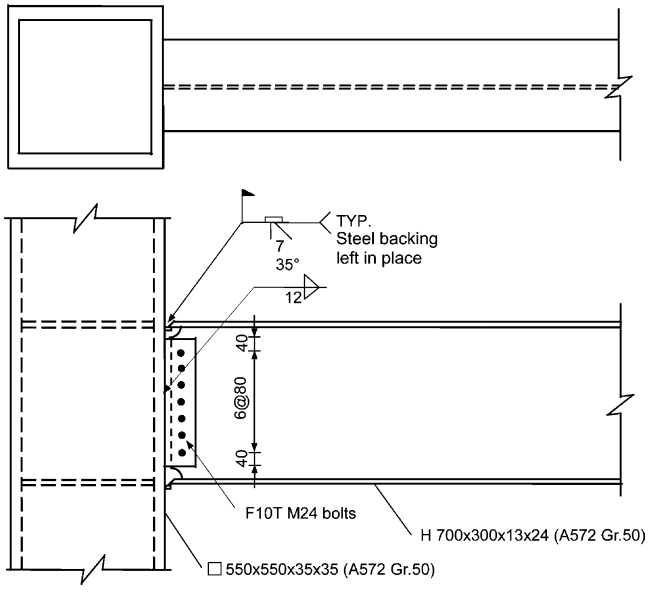

Fig. 6. Connection details of specimen BUN.

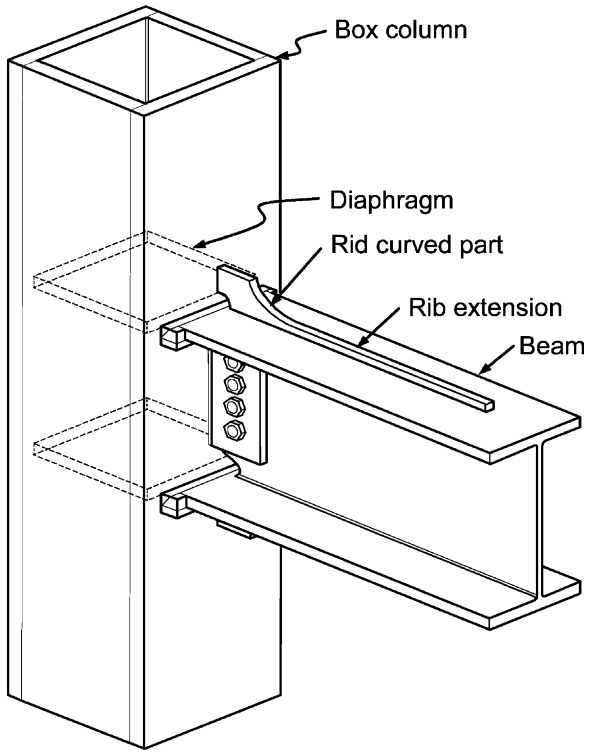

Fig. 7. Schematic of lengthened flange rib connection.

reinforcement afforded by the rib will reduce the stress demand at the CJP weld, and especially the localized stress concentration at the root of the WAH, which cause the beam flange to fracture. The curved part of the flange rib is intended to provide a smooth transfer of forces, while the rib extension is designed to minimize the stress concentrations in the beam flange at the rib end.

3.1.3. *Specimens with rib-reinforced connection*

Five specimens whose connections were reinforced by the flange rib were designed to investigate their hysteretic behaviour. Table 1 presents the design parameters of the specimens. Variously sized rib plates were used to study the effect of reinforcement on the connection behaviour. Based on the capacity design concept, the parameter that governs rib reinforcement at the joint is the ratio of the flexural capacity, M_{cap}, to the moment demand, M_{dem}, as indicated in Fig. 8, and this ratio is defined as the rib reinforcement ratio. The flexural capacity can be calculated as the sum of the flexural strengths of the beam and the rib section at the beam-to-column interface. The moment demand is the required flexural moment at the beam-to-column interface. As indicated by previous studies [26,27], the application of classical beam theory at the joint causes the predictions of the force transferred from the beam to the column to be underestimated. Therefore, for the guarantee that the rib-reinforced connection can pro-

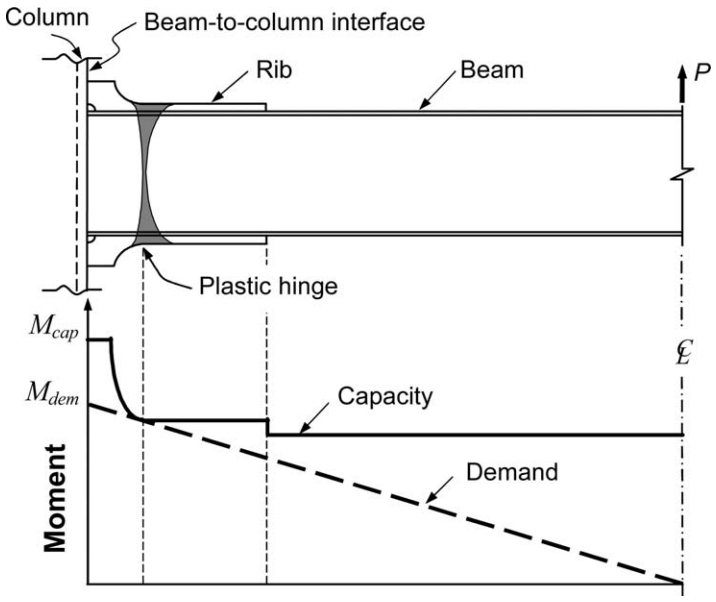

Fig. 8. Moment capacity and demand of lengthened flange rib connection.

vide reliable capacity at the joint, the rib reinforcement ratios used to design the rib plates were raised to 1.05, 1.15 and 1.20, and the specimens were designated by these ratios. Certainly, the higher ratio results in higher margin of safety at the joint.

The backing bar used in the full penetration weld between the beam flange and the column flange creates a notch effect and consequent fracturing of the weld, as was observed during the 1994 Northridge earthquake, so the specimens herein were steel-backed and ceramic-backed to evaluate the effect of such backing. 'SB' and 'CB' stand for steel backing and ceramic backing, used during CJP welding, respectively. 'SB-FW' represents a specimen whose steel backing was supplemented by additional fillet welds to connect to both the beam flange and the column flange. All the steel backing bars were left in place by considering the reinforcement by the rib.

Furthermore, not only was specimen BR120CB-WP reinforced using flange ribs but also it was stiffened by flat wing plates, to prevent a crack from being initiated in the edges of the CJP weld. Figs. 9–11 illustrate the connection details of the rib-reinforced specimens, in which the ribs were fillet welded to the beam flange based on the calculation of shear flow to transmit the horizontal shear forces acting between the rib and the beam. The mechanical properties for all the beams and the columns obtained from tensile coupon tests are presented in Table 2.

3.2. Test setup and loading histories

Fig. 12 depicts the test setup for simulating the seismic loading state of an exterior beam-to-column moment connection in a moment frame. Each specimen was loaded with a 980 kN actuator connected to the free end of the cantilever beam. The actuator was able to move the beam tip 200 mm forward and backward. All specimens were tested under stroke control with the same loading history, as indicated in Fig. 13, following a predetermined cyclic loading history, which was according to the ATC-24 testing protocol [28]. The displacement amplitudes were increased in multiples of the yielding displacement Δ_y, 22 mm, which represents a story drift angle of 0.57%. The Δ_y represents a displacement at the beam tip that causes the beam section to yield. The story drift angle was calculated by dividing the displacement at the beam tip by the distance from the beam tip to the column centerline. Lateral supports were provided to eliminate the lateral deformation of the beam and consequent damage to the actuator.

4. Experimental results

4.1. Global behaviour and failure mode

Specimens' behaviour and failure modes varied with the design of the connections. Table 3 summarizes the failure mechanisms of all of the specimens. Their hysteresis behaviour and failure are briefly described as follows.

4.1.1. Specimen BUN with unreinforced connection

The whitewash began conspicuously flaking from the beam flanges near the CJP weld because the moment was maximum at the joint. Specimen BUN failed in a

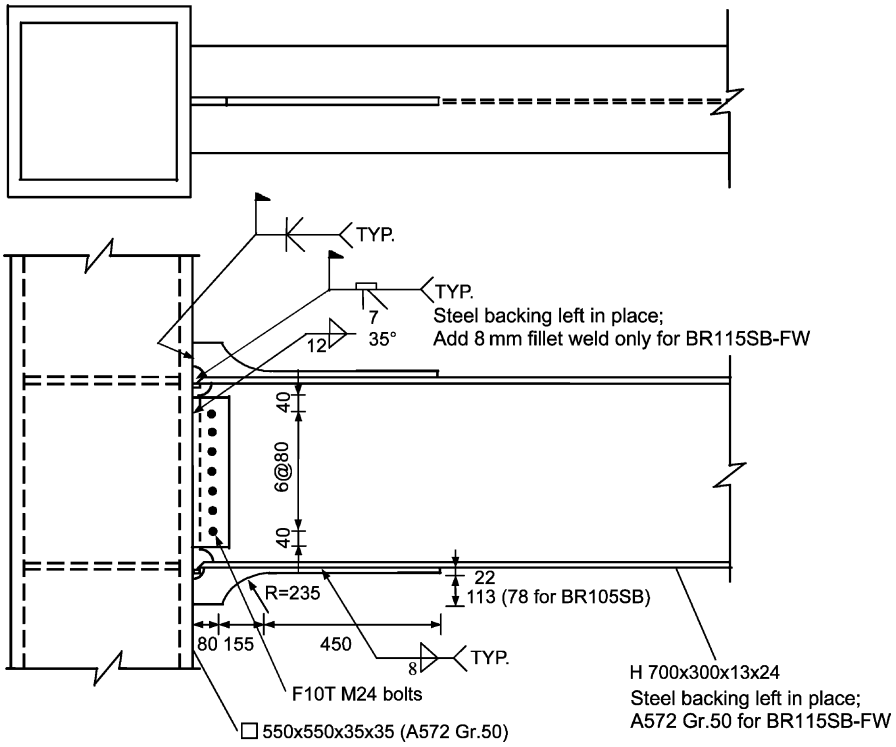

Fig. 9. Connection details of specimens BR115SB, BR105SB, and BR115SB-FW.

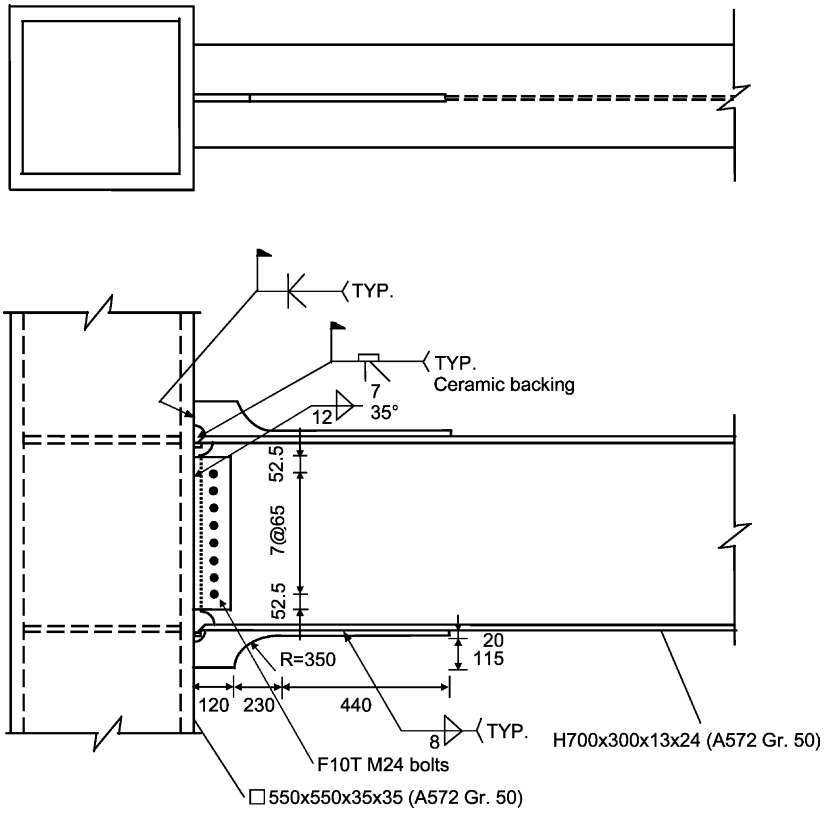

Fig. 10. Connection details of specimen BR115CB.

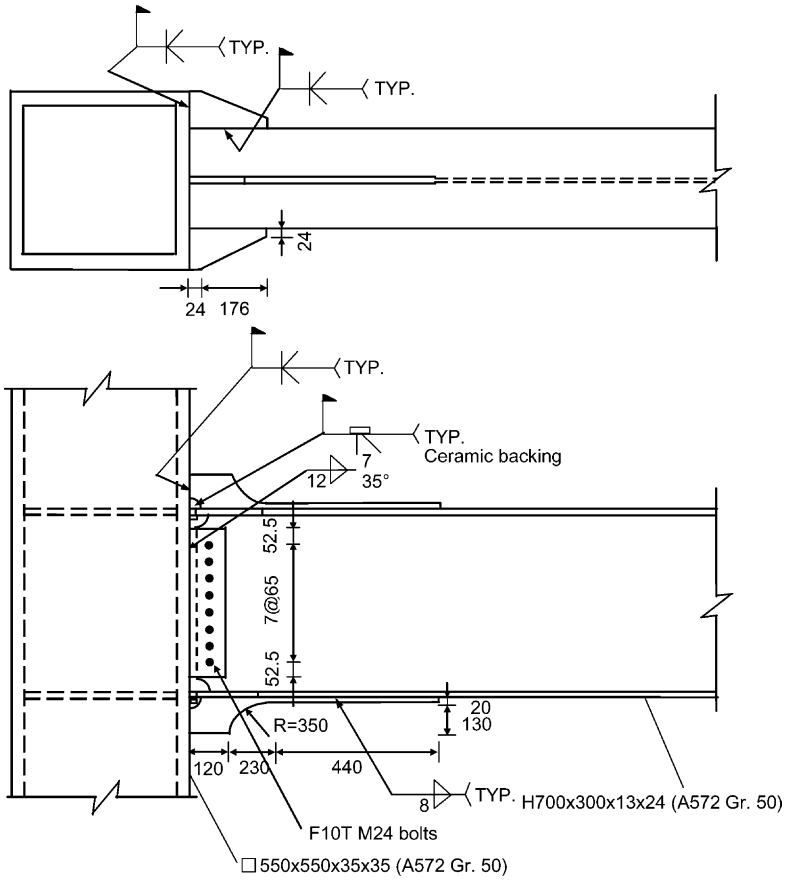

Fig. 11. Connection details of specimen BR120CB-WP.

Table 2
Mechanical properties of test specimens

Specimen	Coupon	Yield strength (MPa)	Ultimate strength (MPa)
BUN	Beam flange	396	516
	Beam web	422	529
	Column plate	412	562
BR115SB	Beam flange	329	465
	Beam web	358	483
	Column plate	421	559
	Rib plate	303	463
BR105SB	Beam flange	329	465
	Beam web	358	483
	Column plate	412	562
	Rib plate	303	463
BR115SB-FW	Beam flange	396	516
	Beam web	422	529
	Column plate	412	562
	Rib plate	319	471
BR115CB	Beam flange	396	516
	Beam web	422	529
	Column plate	421	559
	Rib plate	310	451
BR120CB-WP	Beam flange	396	516
	Beam web	422	529
	Column plate	412	562
	Rib plate	310	451
	Wing plate	403	542

brittle mode with a rapid drop in beam strength caused by the fracturing of the bottom flange of the beam during the 2.3% story drift angle cycle. The cracks originated in the nicks at the root of the CJP flange welds, and propagated rapidly through the beam flange. After the bottom flange had fractured, reverse monotonic loading was exerted to cause the specimen to fail on purpose, to identify the failure mode in the beam top flange. Eventually, fracturing of the beam top flange was initiated in the toe of the WAH, as presented in Fig. 14. This failure demonstrates clearly that the WAH is an indigenous defect of an unreinforced connection, regardless of the geometry of the cross section of the column.

4.1.2. Specimens with rib-reinforced connections

4.1.2.1. Specimen BR115SB. Extensive yielding was observed in beam flanges and the web within the region of the rib extension. This observation is consistent with the objective of the design of the lengthened flange rib. However, cracks were initiated in the CJP weld fusion zone at the edges of the top and bottom flanges of the beam at the first cycle of 3.4% story drift angle. The observation of concentrations of plastic equivalent strains in the finite element analysis, shown in Fig. 4(a),

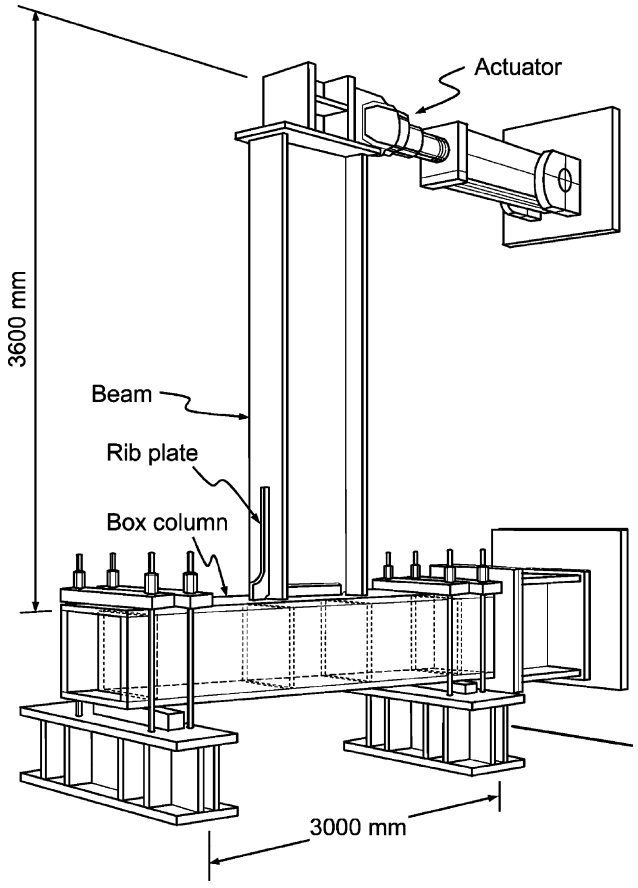

Fig. 12. Test setup.

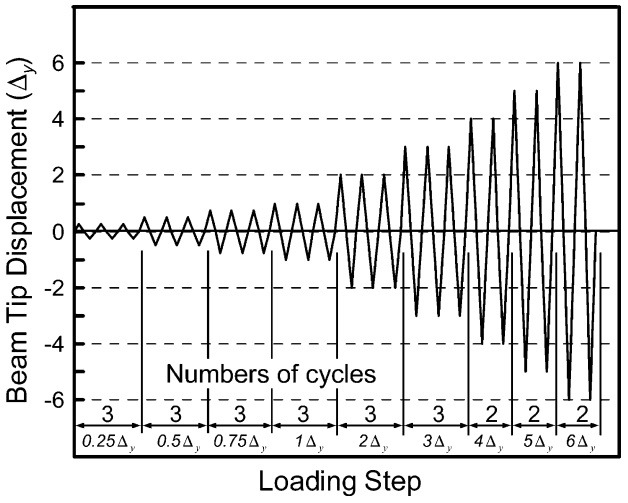

Fig. 13. Loading history.

confirms the formation of these cracks. The primary cause of the failure of specimen BR115SB was the significant local buckling of the beam flanges and the beam web, and slight lateral torsional buckling during the cycles of 4.6% story drift angle, which were followed by the degradation of the strength of the connection. The test was ended after the cycle of 5.1% story drift angle because the excursion limitation of the actuator was reached. Therefore, no fatal damage occurred at the completion of the test. Fig. 15 shows the local buckling of specimen BR115SB at a story drift angle of 5.1%.

4.1.2.2. Specimen BR105SB. The yielding pattern of specimen BR105SB was very similar to that of specimen BR115SB. Yielding in beam flanges within the rib extension was significant during the cycles of 2.3% story drift angle. The plastic hinge that developed in the beam section away from the column face effectively prevented brittle fracture in the CJP groove weld. Minor cracking also occurred in the CJP weld fusion zone at the edges of the beam flange during the cycle of 3.4% story drift angle. Likewise, during the cycles of 4.6% story drift angle, considerable local buckling of the beam section, followed by degradation of strength was observed. After a final cycle of 5.1% story drift

Table 3
Test results of specimens

Specimen	Total plastic rotation θp (% rad)	Description of failure
BUN	+1.10	a. Fracturing of the beam bottom flange
	−2.89	b. Tearing of the beam top flange initiated from the weld access hole
BR115SB[a]	+3.76	a. Local buckling of beam flanges and web followed by slightly lateral torsion buckling
	−4.01	b. Cracking of the complete joint penetration welds on both edges
BR105SB[a]	+3.95	a. Local buckling of beam flanges and web
	−4.01	b. Cracking of the complete joint penetration welds on both edges
BR115SB-FW	+3.30	a. Local buckling of beam flanges and web
	−3.19	b. Fracturing of the beam top flange
BR115CB	+0.00	a. Defect of SESNET welding
	−0.00	b. Fracturing of groove weld in the beam top flange and ribs
BR120CB-WP	+1.71	a. Cracking of wing plates at its tips followed by tearing of the beam bottom flange
	−1.59	b. Cracking of groove welds on the bottom rib

[a] The test was stopped due to the excursion limitation of the actuator.

Fig. 14. Fracture of beam top flange of unreinforced specimen BUN.

angle, test was terminated due to the excursion limitation of the actuator. No brittle fracture was observed either at the weld joints or in the WAH region during the test. Fig. 16 shows the local bucking in the beam of specimen BR105SB at 5.1% story drift angle.

4.1.2.3. Specimen BR115SB-FW. Further fillet welds were added to specimen BR115SB-FW to join the steel backing to both the beam flange and the column flange to eliminate the possible notch effect associated with the steel backing. Minor cracking, however, was initiated in the weld fusion zone at the edges of the top flange of the beam. The test outcomes implied that

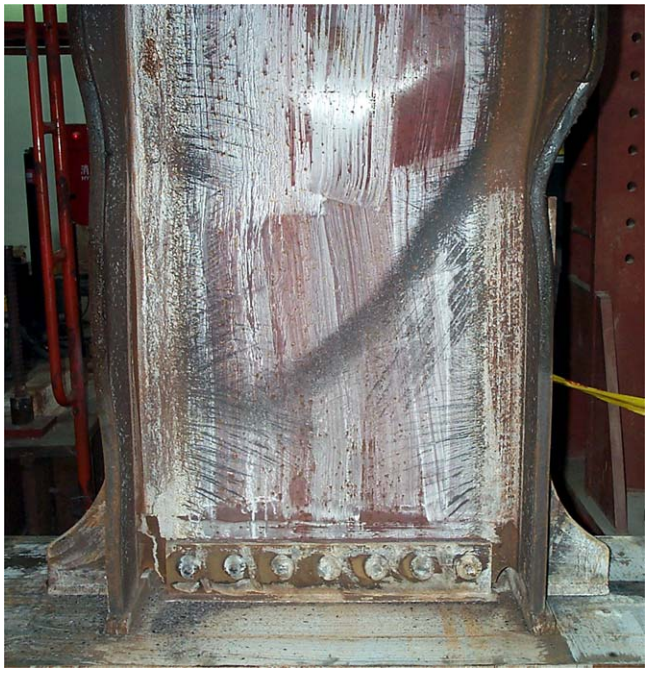

Fig. 15. Local buckling of specimen BR115SB.

Fig. 16. Local buckling of beam flange and web of specimen BR105SB.

these additional fillet welds could share some of the stresses and prevent initial cracking that would otherwise originate under the top flange of the beam, as illustrated in Fig. 17. However, these additional fillet welds cannot satisfactorily prevent cracking at the CJP weld. The crack finally led to the beam flange to fracture. The test was ended because the beam top flange tore at the final excursion of 4.6% story drift angle.

4.1.2.4. Specimen BR115CB. Specimen BR115CB exhibited the worst performance of all of the rib-reinforced specimens. The failure of this specimen was due to fracture of the groove weld that joined the beam top flange and the rib plate to the column flange, as shown in Fig. 18. The fracture originated in the tips of the weld metal near the beam flange, and propagated to the base metal of the column plate, during the cycles of 1.7% story drift angle. The specimen eventually failed without developing plastic flexural strength of the beam. Specimen BR115CB differed from specimen BR115SB only in the ceramic backing used in the former. Therefore, a further inspection was undertaken to discover the causes of the failure. The column flange plates were removed to examine the welding of the diaphragms. Flaws were found at the weldment of the SESNET welding process; however, ultrasonic testing did not reveal the defect. The flaws of the weldment caused the column flange to separate from the diaphragm, resulting in out-of-plane deformation and consequent fracture of the column flange.

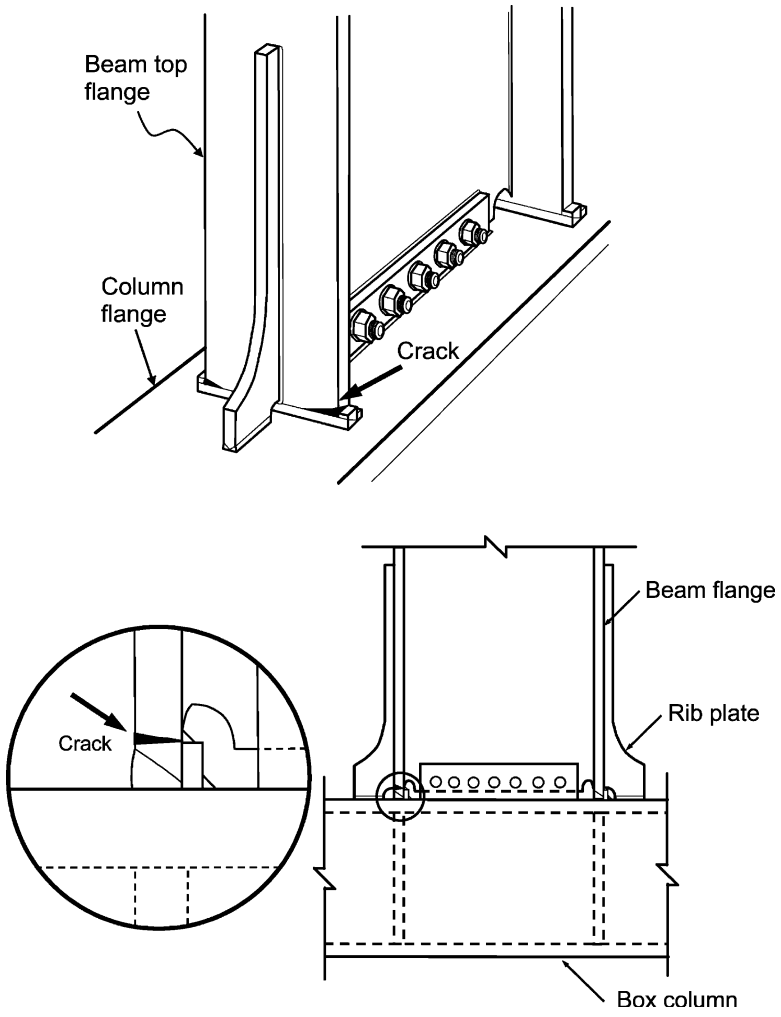

Fig. 17. Failure of specimen BR115SB-FW.

4.1.2.5. Specimen BR120CB-WP. This specimen was further reinforced by welding flat wing plates in addition to the rib plates, to reduce the concentration of stress at both edges of the flange groove weld. Premature cracks were noticed at the end tip of the weldment that connected the wing plates to the beam flange at the cycle of 1.1% story drift angle. This cracking propagated further toward the beam flange as the beam tip displacement increased. One of the wing plates separated from the beam flange at a story drift angle of 2.9%. Fig. 19 illustrates the locations of the cracks. The test was terminated at the cycle to 3.4% story drift angle because the tearing of the beam flange and the failure of the weldment drastically reduced the beam strength. This brittle fracturing may have been caused by the concentration of stresses at the tips of the wing plates, due to the geometric discontinuity.

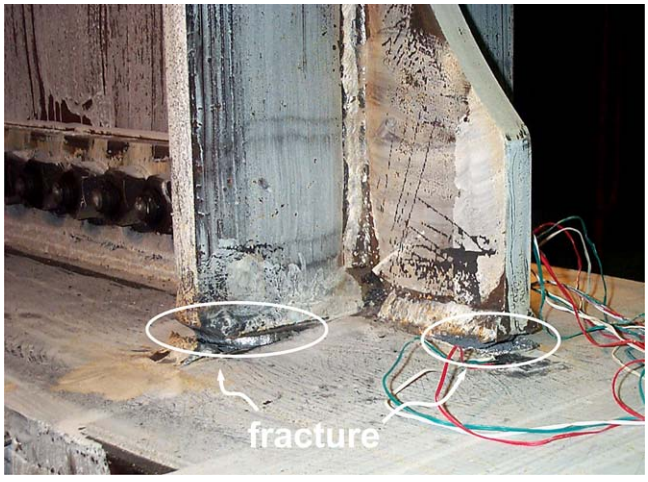

Fig. 18. Fracture of CJP groove weld of specimen BR115CB.

4.2. Hysteretic response

Hysteresis curves of moment versus total plastic rotation of all specimens are presented in Fig. 20. The

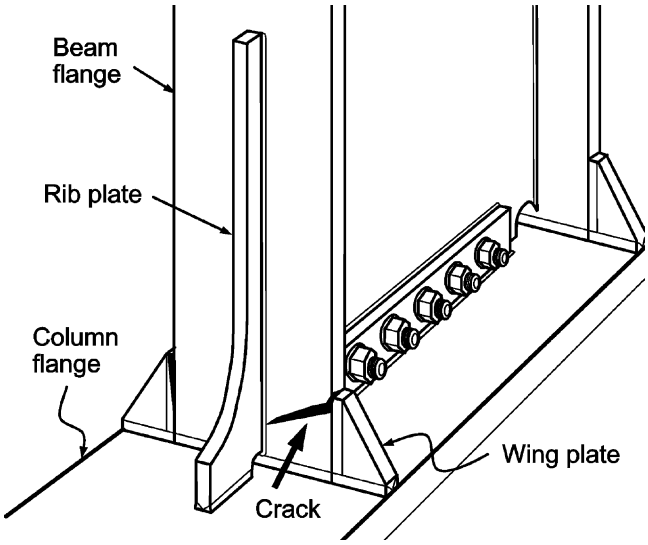

Fig. 19. Tearing of beam flange of specimen BR120CB-WP at 3.4 story drift angle.

moment is computed by multiplying the beam loading by the distance from the beam tip to the column face. In the figures, the moments are also normalized to plastic flexural strength of the beam section, which is determined from the strength measured in coupon tests. The total plastic rotation is calculated by subtracting the angle of elastic rotation from the total angle of rotation. Table 3 summarizes the maximum total plastic rotations of all specimens; the angles of total plastic rotation are in the range 1.10–4.01% rad. The inelastic deformation of the beam section contributes to plastic rotation because the column and the panel zone behaved elastically during the test, calculated based on the data recorded from the instrumentation. Notably, a plastic rotation of over 3% rad is required to qualify for a steel special moment-resisting frame in the 1997 AISC seismic provisions [29] and in Taiwan.

Fig. 20(a) shows the hysteresis curve of specimen BUN. This specimen developed a plastic rotation of 1.1% (with failure at the beam bottom flange) and −2.89% rad (with failure at the beam top flange). Higher plastic rotation was obtained, compared to the specimens done by Kim et al. [15]. Here, the rotational capacity implies that the BWWF unreinforced connection with this specific WAH configuration cannot satisfy the requirement for a moment connection used in the seismic load resisting system. Nevertheless, the tests done by Ricles et al. [20] showed that unreinforced connection with a modified WAH geometry and a welded beam web can reliably develop a satisfactory inelastic rotation. It should be noted that all their connections used an H-shaped column. It is of great interest to see whether the modification can improve the behaviour of the connection with box column.

Specimens BR115SB, BR105SB and BR115SB-FW, reinforced by the flange rib, exhibited considerably improved hysteretic behaviour, as indicated in Fig. 20(b)–(d). They all behaved very similarly, independently of their various size ribs. The curves show stable, reliable cyclic loops. Hysteresis loops demonstrate gradual deterioration in the flexural strength under the influence of local buckling at the beam flanges and the web; however, the flexural strength still exceeds the plastic flexural strength of the beam. All three specimens exhibited plastic rotation of more than 3% rad, despite their two different rib reinforcement ratios of 1.05 and 1.15.

Fig. 20(e) shows the hysteresis loop of specimen BR115CB, which reveals the unexpected failure of the connection due to a welding defect in the diaphragm. The flexural strength of this specimen did not even reach the plastic flexural strength of the beam because the poor SESNET welding caused the beam flange to fracture. The quality of the SESNET welding to join the diaphragm inside the box column is crucial to the transfer of the beam forces to the connection. The performance of the connection depends greatly on the integrity of the diaphragm and the column plates.

Fig. 20(f) demonstrates the hysteresis curve of specimen BR120CB-WP. The fracturing of the beam flange from its junction with the wing plate during early loading cycles led to a significant loss of the strength, causing unsatisfactory cyclic behaviour.

The effect of the ceramic backing on the performance of the CJP weld is unclear from the tests of specimens BR115CB and BR120CB-WP, because both specimens failed prematurely since the SESNET welding was defective in specimen BR115CB and a crack was initiated at the tips of the wing plates in specimen BR120CB-WP.

4.3. Verification of effectiveness of flange rib application

Variations of flexural moment along the length of the beam are examined to further verify the efficacy of the lengthened flange rib. The degree of yielding of the beam section can be determined by comparing the test moment to the flexural capacity of the beam. Two critical locations are of interest—the beam-to-column interface and the plastic hinge. Accordingly, the maximum test moment, M_{test}, is defined as the maximum testing load multiplied by the distance from the beam tip to either the beam-to-column interface or the location of the plastic hinge. Fig. 21 plots the ratios of the maximum test moment to the plastic flexural capacity of the beam, including the rib plates, M_{test}/M_p, for the three flange rib-reinforced specimens. The ratios at the interface are in the range 1.02–1.09, implying

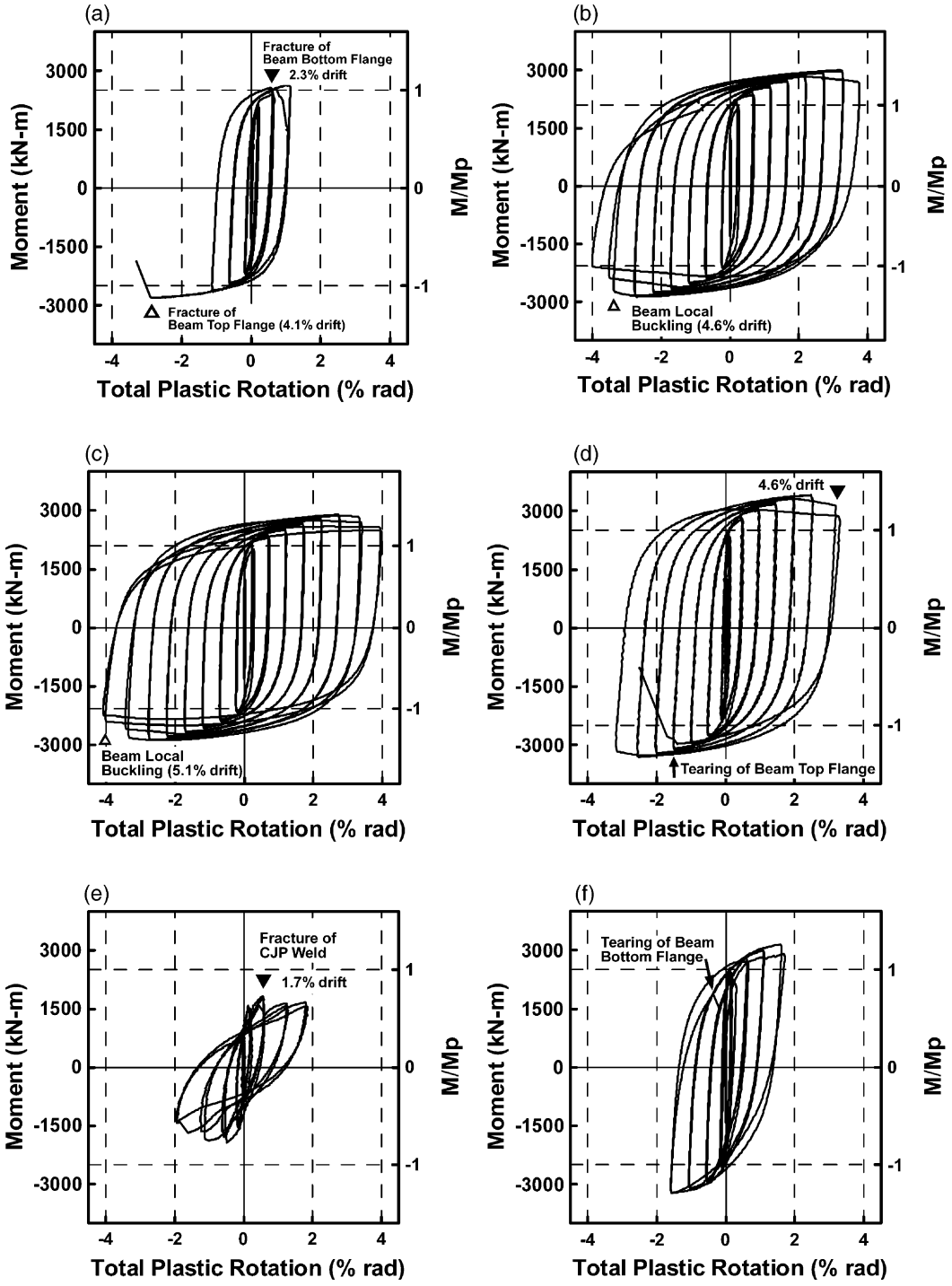

Fig. 20. Moment versus total plastic rotation relationships: (a) specimen BUN; (b) specimen BR115SB; (c) specimen BR105SB; (d) specimen BR115SB-FW; (e) specimen BR115CB; (f) specimen BR120CB-WP.

that the test moments barely reach the plastic flexural capacity of the beam at the beam-to-column interface. Meanwhile, the ratios at the location of the plastic hinge range from 1.20 to 1.24, indicating that the beam yielded at the location of the plastic hinge and the beam sections were stressed into the strain-hardening range. These limited test results imply that specimens reinforced using a lengthened flange rib cannot merely reduce the stress demand at the beam-to-column interface, but also develop a plastic hinge in the beam section away from the face of the column. However, further study is needed to utilize the ribs in various beam and column size.

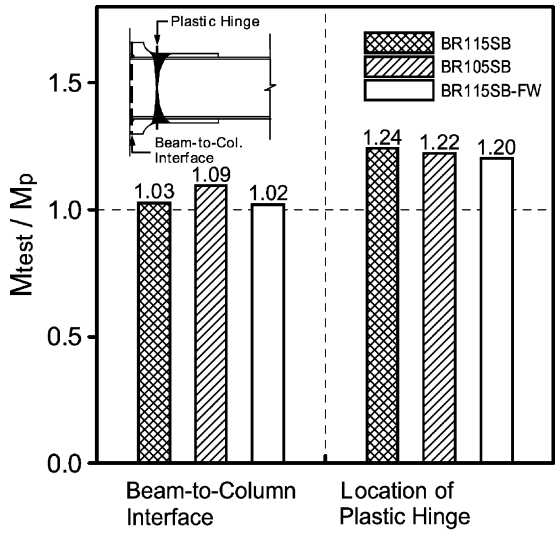

Fig. 21. Ratios of flexural moment to plastic flexural capacity.

5. Conclusions

This study involved an experiment to address the seismic performance of connections between a steel beam and a welded box column. The analytical and experimental results presented herein support the following conclusions.

1. In the connection with the box column, local stresses and plastic equivalent strains peak at the edges of the CJP weld and in the WAH region, as revealed by finite element analysis, which is different from those of the connection with an H-shaped column.
2. The unreinforced connection failed due to fracture at the CJP weld and near the WAH region. These are the locations of the peak local stresses and plastic equivalent strains predicted by finite element analysis. The test outcomes for specimen BUN revealed that this unreinforced connection with a quarter-circular shape WAH is vulnerable, and that brittle failure was caused by the localized stress concentrations. However, other improving schemes, such as a modified WAH geometry or a welded beam web, may result in a different behaviour.
3. Although the limited number of tests has been conducted in this study, the test results of three connections reinforced with the lengthened flange rib demonstrated that reinforcement can significantly improve the hysteretic behaviour of the connection, to achieve a plastic rotation of at least 3% rad. Additional research should be done to further apply to different sizes of beams and columns, and to further develop design recommendation for rib-reinforced connection.
4. Lengthened flange rib plates can prevent brittle cracking at the beam-to-column joint, cause stable yielding in the beam section away from the weld fusion zones, and result in reliable inelastic deformation.
5. The specimen reinforced by additional flat wing plates exhibited premature failure due to the localized stress concentration at the tips of the wing plates.

Acknowledgements

The authors would like to thank the Sinotech Engineering Consultants, Inc. for financially supporting this research.

References

[1] Miller DK. Lessons learned from the Northridge earthquake. Engineering Structures 1998;20(4–6):249–60.
[2] Lu LW, Ricles JM, Mao C, Fisher JW. Critical issues in achieving ductile behaviour of welded moment connections. Journal of Constructional Steel Research 2000;55:325–41.
[3] Stojadinovic B, Goel SC, Lee KH, Margarian AG, Choi JH. Parametric tests on unreinforced steel moment connections. Journal of Structural Engineering, ASCE 2000;126(1):40–9.
[4] Maranian P. Vulnerability of existing steel framed buildings following the 1994 Northridge (California, USA) earthquake: considerations for their repair and strengthening. The Structural Engineer 1997;75(10):165–72.
[5] Engelhardt MD, Sabol TA. Reinforcing of steel moment connections with cover plates: benefits and limitations. Engineering Structures 1998;20(4–6):510–20.
[6] Uang CM, Bondad D, Lee CH. Cyclic performance of haunch repaired steel moment connections: experimental testing and analytical modeling. Engineering Structures 1998;20(4–6):552–61.
[7] Kim T, Whittaker AS, Gilani ASJ, Bertero VV, Takhirov SM. Experimental evaluation of plate-reinforced steel moment-resisting connections. Journal of Structural Engineering, ASCE 2002;128(4):483–91.
[8] Engelhardt MD, Winneberger T, Zekany AJ, Potyraj TJ. Experimental investigation of dogbone moment connections. Engineering Journal, AISC 1998;35(4):128–39.
[9] Popov EP, Yang TS, Chang SP. Design of steel MRF connections before and after 1994 Northridge earthquake. Engineering Structures 1998;20(12):1030–8.
[10] Chen SJ, Yeh CH, Chu JM. Ductile steel beam-to-column connections for seismic resistance. Journal of Structural Engineering, ASCE 1996;122(11):1292–9.
[11] Lee SL, Ting LC, Shanmugam NE. Use of external T-stiffeners in box-column to I-beam connections. Journal of Constructional Steel Research 1993;26:77–98.
[12] Shanmugam NE, Ting LC. Welded interior box-column to I-beam connections. Journal of Structural Engineering, ASCE 1995;121(5):824–30.
[13] Dawe JL, Grondin GY. W-shape beam to RHS column connections. Canadian Journal of Civil Engineering 1990;17:788–97.
[14] Shanmugam NE, Ting LC, Lee SL. Behavior of I-beam to box-column connections stiffened externally and subjected to fluctuating loads. Journal of Constructional Steel Research 1991;20:129–48.
[15] Kim T, Stojadinovic B, Whittaker AS. Seismic performance of US steel box column connections. Proceedings, 13th World Conference on Earthquake Engineering, Canada, 2004, Paper No. 981.

[16] Kim T. Experimental and analytical performance evaluation of welded steel moment connections to box or deep W-shape columns. PhD dissertation, University of California, Berkeley, CA, 2003.
[17] Roeder CW. General issues influencing connection performance. Journal of Structural Engineering, ASCE 2000;128(4):420–8.
[18] ANSYS User Manual. ANSYS, Inc., 2001.
[19] EI-Tawil S, Mikesell T, Kunnath SK. Effect of local details and yield ratio on behavior of FR steel connections. Journal of Structural Engineering, ASCE 2000;126(1):79–87.
[20] Ricles JM, Mao C, Lu LW, Fisher JW. Inelastic cyclic testing of welded unreinforced moment connections. Journal of Structural Engineering, ASCE 2002;128(4):429–40.
[21] American Institute of Steel Construction. Manual of steel construction: load and resistance factor design, 3rd ed. Chicago (IL): AISC; 2001.
[22] Popov EP, Tsai KC. Performance of large seismic steel moment connections under cyclic loads. Engineering Journal, AISC 1989;26(2):51–60.
[23] Engelhardt MD, Sabol TA, Aboutaha RS, Frank KH. Testing connections. Modern Steel Construction, AISC 1995;35(5):36–44.
[24] Anderson JC, Duan X. Repair/upgrade procedures for welded beam to column connections. Report No. PEER 98/03, Pacific Earthquake Engineering Research Center, Richmond (Ca), 1998.
[25] Chen CC, Lee JM, Lin MC. Behaviour of steel moment connections with a single flange rib. Engineering Structures 2003;25(11):1419–28.
[26] Goel SC, Stojadinovic B, Lee KH. Truss analogy for steel moment connections. Engineering Journal, AISC 1997;34(2): 43–53.
[27] Lee CH. Seismic design of rib-reinforced steel moment connections based on equivalent strut model. Journal of Structural Engineering, ASCE 2002;128(9):1121–9.
[28] ATC. Guidelines for seismic testing of components of steel structures. Report ATC-24, Applied Technology Council, Redwood City (CA), 1992.
[29] American Institute of Steel Construction. Seismic provisions for structural steel buildings. Chicago (IL): AISC; 1997.